Journal of Dynamic Systems, Measurement and Control. Received September 30, 2020;
Accepted manuscript posted January 18, 2021. doi:10.1115/1.4049796

Modeling of a Fractional Order Element Based on Bacterial Cellulose and Ionic Liquids

R. Caponetto, S. Graziani, E. Murgano and C. Trigona
DIEEI
University of Catania
Italy
Email: riccardo.caponetto@unict.it

A. Pollicino
DICAR
University of Catania
Italy
Email: apollicino@unict.it

G. Di Pasquale
DSC
University of Catania
Italy
Email: gdipasquale@unict.it

In this paper, a novel Fractional-Order Element (FOE) is modelled in a wide frequency range. The FOE is based on a green bio-polymer, i.e., Bacterial Cellulose (BC), infused with Ionic Liquids (ILs). The modelling is performed in the frequency domain and a lumped-circuit model is proposed. The model is an evolution with respect to a simpler one already introduced by the authors, for a narrower frequency range. Results show that ILs generate a quite complex frequency domain behaviour, which can be described in the framework of FOEs. Furthermore, results on the time stability of the device under investigation are given.

1 Introduction

The scientific community has the responsibility to switch from the present grey economy to a greener economy [1]. New technologies are therefore required to improve human-beings quality of life in the respect of the environment. Precision Agriculture (PA), Internet of Food (IoF), or Smart Cities (SC) can give a relevant contribution to achieve a sustainable growth. New technologies need to focus on a smarter use of resources. In the electronics field, this goal can be translated into the realization of new devices with new functionalities, low commercial costs, and furthermore, an eco-friendly production.

Because of the envisaged low cost, new electronics devices will have an ever and ever reduced utilization life and this could lead, unfortunately, to the increasing of electronics-wastes, *e-wastes*, difficult to dispose. It is estimated that $44.7 \cdot 10^9$ *kg* of *e-wastes* has been produced in 2016, [2] - an equivalent of almost 4500 Eiffel towers, while in 2018 its production has achieved an amount of approximately $50 \cdot 10^9$, see [3]. Only 20% of this is formally recycled [4]. Such an huge amount of *e-wastes* is very complicated to dispose, not only because of the logistic, but also, and above-all, because of the environmental impact. Indeed, electronic devices can release dangerous chemical matters into the environment, if they are not correctly disposed. Such a scenario can affect both the environment and human being healthiness.

A possible solution to this issue can be represented by the development of new production technologies, which require using less energy and less polluting materials, preferring renewable energy sources and recyclable or biodegradable materials.

Research is focusing on the most common biopolymer on Earth, i.e., cellulose, [5]. It is biocompatible and biodegradable and, although it is usually produced by plants, a new kind of cellulose, Bacterial Cellulose (BC), produced by bacteria, has created a lot of interest in many research fields (e.g. electronics, material science), due to its unique properties, [6, 7]. BC has the same chemical formula of its plant-derived counterpart but, thanks to its unique nature, it can be produced in typical laboratory conditions, without an excessive use of water, energy, or other non eco-friendly procedures, which are required by the pulp industry. BC can be produced by commercial tea bags, sucrose, bacteria and yeast strain, , and acetic acid. Sodium hydroxide is used for the final product purification, see [8].

BC has been proposed for realizing composites capable of both mechanoelectrical and electromechanical transduction capabilities. These have been exploited to realize sensors [9, 10], power harvesters [11], and actuators [12, 13].

Along with environmental issues, research for new electronics needs to realize and implement new functionalities. An important active area deals with the realization of Fractional-Order Elements (FOEs) [14, 15], i.e. elements whose behaviour can be represented by means of the

Journal of Dynamic Systems, Measurement and Control. Received September 30, 2020;
Accepted manuscript posted January 18, 2021. doi:10.1115/1.4049796

Fractional-Order Calculus (FOC) [16,17]. More specifically, FOEs can be defined as a generalization of the well-known Constant Phase Elements (CPEs), which have been studied since decades and used to model, e.g., electrochemical reactions and electrode impedance. These elements show a constant-phase over a wide frequency range and this behaviour can be defined as the building block to develop fractional-order electronics [18].

The most widely investigated FOE is the fractional capacitance. A fractional-order capacitance can be defined by the following equation:

$$Z(s) = \frac{1}{s^{\alpha} C} \tag{1}$$

where α is the fractional order and C is the pseudo-capacitance. The unit of C is $F/s^{1-\alpha}$ [19].

Eq. (1) can be thought as a generalization of the impedance of the well-known integer-order capacitance, which is obtained by imposing $\alpha = 1$. It is quite evident that the possibility of defining an arbitrary value of α allows us to introduce new and more flexible electronics. Combining the two aforementioned research fields, the possibility of realizing new devices with new functionalities in an eco-friendly way emerges.

Recently it has been shown that BC can be used to realize FOEs [14]. Also the possibility of changing the behaviour of BC based FOEs by exploiting Ionic Liquids (ILs) has been introduced in [20].

In this paper, new results on the modelling of this latter class of BC-based composites, indicated in the following as BC-IL-FOEs, are reported. The behaviour of BC-IL-FOEs is investigated in a wide frequency range. A lumped equivalent circuits are used to model the BC-IL-FOEs. More specifically, models of different complexities are considered and their performance are compared. Finally, a long lasting experimental measurement campaign has been executed with the aim of investigating device time instabilities.

The paper is organized as follows: in Section 2, a brief overview on FOC and FOEs is given. In Section 3, the fabrication of the BC-IL-FOEs is discussed. In Section 4, the experimental setup is shown, while in Sections 5 and 6 results and conclusions are drawn, respectively.

2 A brief overview on FOC theory and FOEs realization

An $\alpha - th$ order derivative or integral, with $\alpha \in \mathbb{R}$ can be evaluated by exploiting the FOC. The non integer-order operator ${}_a\mathscr{D}_t^{\alpha}$ with $a, t \in \mathbb{R}$ as operation limits, is defined as follows:

$${}_a\mathscr{D}_t^{\alpha} = \begin{cases} \frac{d^{\alpha}}{dt^{\alpha}} & : \alpha > 0 \\ 1 & : \alpha = 0 \\ \int_a^t (d\tau)^{-\alpha} & : \alpha < 0 \end{cases} \tag{2}$$

Three different definitions can be used to compute the previous operator. For the continuous time domain, these are the Riemann-Liouville (*RL*) and Caputo (*CP*), while, in the discrete case, the Gründwald-Letnikov (*GL*) can be used [21].

The *RL* and *CP* definitions for a function $f(t)$ are defined, respectively, as:

$$\{{}_a\mathscr{D}_t^{\alpha}\}_{RL} f(t) = \frac{1}{\Gamma(n-\alpha)} \frac{d^n}{dt^n} \int_a^t \frac{f(\tau)}{(t-\tau)^{\alpha-n+1}} d\tau, \tag{3}$$

and:

$$\{{}_a\mathscr{D}_t^{\alpha}\}_{CP} f(t) = \frac{1}{\Gamma(n-\alpha)} \int_a^t \frac{f^{(n)}(\tau)}{(t-\tau)^{\alpha-n+1}} d\tau, \tag{4}$$

where $n \in \mathbb{Z}: \ n-1 < \alpha \leq n$ and $\Gamma(\cdot)$ is the *Euler Gamma* function.

Although (3) and (4) appear quite similar, the *CP* definition is more used because, in the Laplace domain, the initial condition still maintains a physical meaning, while with the *RL* one this does not occur.

The *GL* definition is given by the following relation:

$$\{{}_a\mathscr{D}_t^{\alpha}\}_{GL} f(t) = \lim_{h \to 0} h^{-\alpha} \sum_{j=0}^{[\frac{t-a}{h}]} (-1)^j \binom{\alpha}{j} f(t - jh), \tag{5}$$

where $[\cdot]$ evaluates the integer part of its argument.

Only in the last decades the FOC has been applied in many research areas [22], like automatic control [23, 24], electronic implementation [25], medical applications [26], electrochemistry, economics [27], and civil engineering [28].

Strictly related to FOC, another practical and interesting application can be found in the realization of FOEs: i.e., the realization of devices that have, as their intrinsic nature, a fractional-order behaviour. Different technologies have been proposed to realize FOEs and, more specifically, CPEs. They can be clustered in the following three main classes: multi-components, emulated, and single-components [29]. The latter class is of interest because it allows us to develop compact devices that could be used in real application. The largest sub-family of single-components are the solid-state FOEs. These can be further divided, according to the implementing technologies, as graphene-polymer dielectric [30], carbon black-polymer dielectric [31], and MoS_2-polymer composites [32], Carbon Nano Tubes [33], and Ionic Polymer Metal Composites [34].

3 BC-based FOEs

BC-based FOEs have been proposed by the authors [14]. In that contribution bacterial-derived cellulose is used as the dielectric of a Cu-parallel plates capacitor.

In a successive contribution, the authors investigated the possibility of modulating the behaviour of BC-based FOEs

Journal of Dynamic Systems, Measurement and Control. Received September 30, 2020;
Accepted manuscript posted January 18, 2021. doi:10.1115/1.4049796

by means of ILs [20]. In this paper, the performance of this latter device is analysed in a wide frequency range and a model, in the form a lumped element circuit, is proposed.

The BC used to realize the BC-IL based FOE described in the following of this paper was produced by a culture of Acetobacter xylinum and was purchased by Biofaber s.r.l., in the form of dehydrated sheets of about $(23 \times 28 \times 0.04)$ cm.

Details about the BC production procedure adopted by the supplier can be found in [8].

1-Ethyl-3-Methylimidazolium Trifluoromethanesulfonate (EMIM-TFMS), used as the IL (melting temperature $-13\ ^{\circ}C$), was purchased from Alfa Aesar. BC pieces were dried and were then soaked with EMIM-TFMS for 24 h. Finally they were dried in a vacuum oven for 2 h at 65 $^{\circ}C$.

The IL uptake, calculated by comparing the weights of the IL-treated sample and the dried one, was about 34% by weight. The high IL uptake is due to the tendency of the anion component of the IL to strongly coordinate to the carbohydrates' hydroxyl groups of BC. This produces a disruption of inter and intra-molecular hydrogen bonding between cellulose fibrils [35]. Because of this strong interaction, cellulose fibrils are easily wetted by ILs that diffuse into the whole polymer matrix, causing its swelling and the partial hydrolysis on surface.

In order to investigate the BC-IL based FOE, a square of roughly $6 \times 6\ mm^2$ has been cut from the original sheet. FR4 has been used to realize rigid electrodes.

The BC, imbibed with EMIM-TFMS, and the electrodes used to realize the capacitor are reported in Fig. 1.

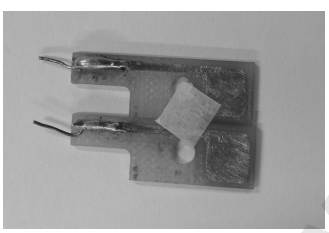

Fig. 1: BC-IL and Cu-electrodes, realized using FR4 card.

4 Experimental setup and results

It has already been outlined that BC-based FOEs are sensible to both humidity and temperature [20]. To avoid such undesired effects, the BC-IL-based FOE has been wrapped with a polyethylene sheet to keep constant as much as possible the relative humidity. In addition, the device has been put inside a polysterene box, in order to reduce as much as possible any temperature fluctuation. The BC-IL-based device, depicted in Fig. 2, has been stored in a temperature-controlled chamber at $T_c = 10\ ^{\circ}C$ when non used for experimental surveys. Only the electrical connections emerge from the box. In order to assure constant working conditions, one measurement per day was performed.

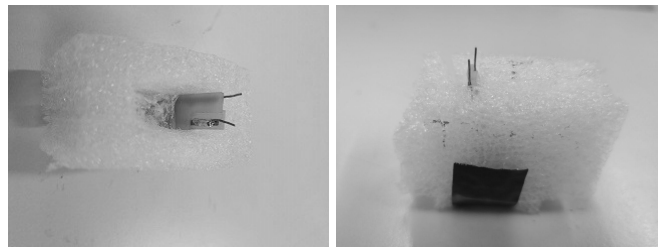

(a) Sealed BC-IL-based FOE (b) Encapsulated BC-IL-based FOE

Fig. 2: BC-IL-based FOE under investigation

The experimental measurements have been performed using a Keysight Network Analyzer E5061B. Both the module and the phase of the device impedance were measured. A logarithmic sweep in the frequency range $[5, 30 \times 10^6]$ Hz has applied. The Intermediate Frequency BandWidth (IFBW) was set to 100 Hz, considering 201 points logarithmically distributed along the investigated frequency range. Finally, an averaging factor equal to 16 was fixed.

In Fig. 3, the probe and its connection to the Network Analyzer are shown, while, in Fig. 4, a screenshot of a measurement in the range $[5; 30 \times 10^6]$ Hz of the Device Under Test (DUT), is reported. Due to inductive parasitic effects which can be noticed at the higher frequency range, the investigation of the DUT has been limited to the range $[5, 1 \times 10^6]$ Hz.

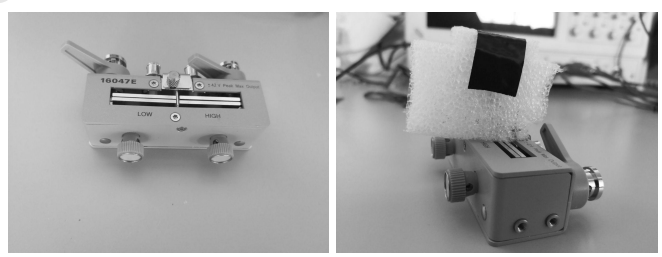

(a) Probe 16047E (b) BC-IL-based FOE mounted in the probe

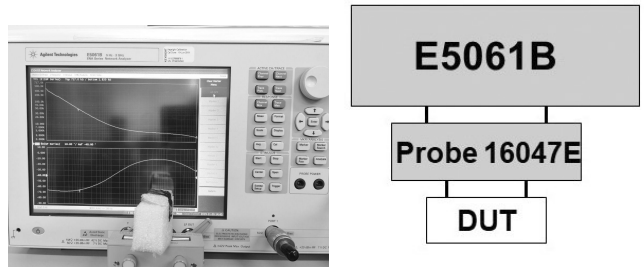

(c) Measurement of BC-IL-based impedance with Network Analyzer E5061B (d) Connecting scheme of the device with the instrumentation

Fig. 3: Probe and electric schematics used for the measurements.

Journal of Dynamic Systems, Measurement and Control. Received September 30, 2020;
Accepted manuscript posted January 18, 2021. doi:10.1115/1.4049796

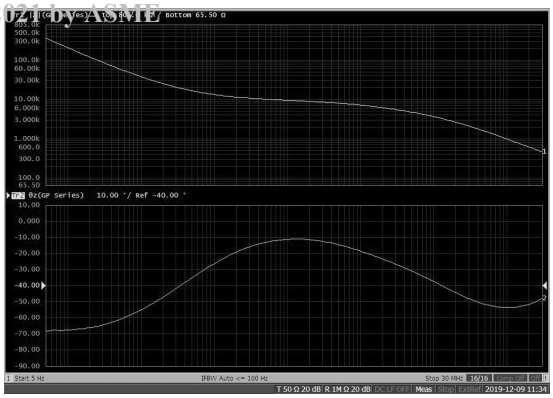

Fig. 4: Screenshot of a generic measurement where both module (top) and phase (bottom) of the impedance are depicted.

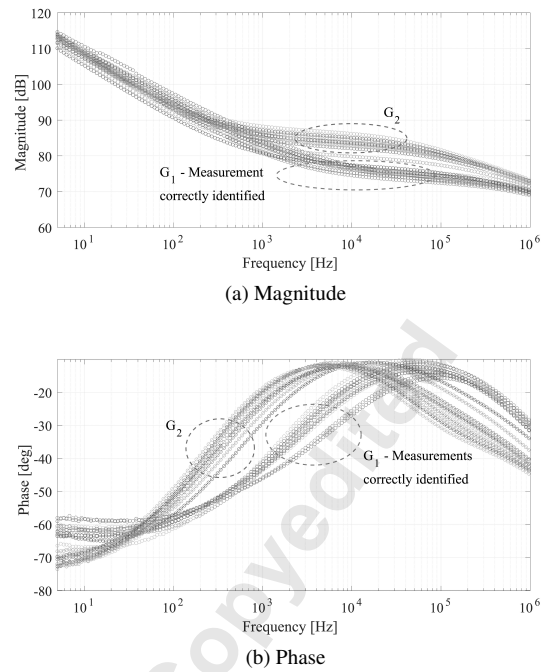

Fig. 5: Bode diagrams of the twenty different measurements. The measurements grouped by the G_1-ellipses will be considered in the following.

The results of twenty different measurements, performed at nominally identical operating conditions and in a long time interval, about 160 d (3900 h), are reported in Fig. 5. It is possible to observe that the behaviour of the DUT derives over time. More specifically, two clusters of curves can be recognized in the figure. The first group (10 curves), labelled as G_1, contains measurements performed during the first month (700 h). The second group, labelled as G_2, contains all the remaining measurements. It is, also, possible to observe that the first group of curves has almost a constant phase, see [29], from the lowest investigated frequency value to about 1 kHz. Such a behaviour is in accordance with results already given by the authors in [20].

As a further consideration, when attempting to model the measurements belonging to the second class, some parameters of the models suffered for lack of stability (see, e.g., the trend of α and β, which will be shown in Fig. 8).

For this reason, though the investigation will be performed on the whole set of available measurements, only the measurements belonging to the first group, indicated by a ellipses in Fig. 5, will be considered for an in deep investigation.

5 Modeling

A model for the BC-IL-based device, in the low-frequency range, has been already proposed [20]. In particular, a fractional-order RC^{α} circuit was proposed. Such a model can not fit the measured magnitude and phase diagrams reported in Fig. 5. A more general model is, therefore, required.

Nyquist plots are generally used to study the ionic conductivity of polymeric electrolytes. Fig. 6 shows a Nyquist plot of te impedance measured for the BC-IL-based FOE under investigation (the first measurement among the entire set). In particular, the circular-like behaviour is due to high-frequency phenomena, while the straight line corresponds to the low-frequencies [36]. Fig. 6 deviates from the ideal case, where a semicircle should be obtained at high frequencies, and a vertical line should characterize the low frequency range. Such discrepancies, probably due to diffusion of the mobile charges inside the composite, can be accounted for if equivalent circuits consisting of combinations of CPEs are used.

Taking into account these considerations, a possible model to explain all the diffusive phenomena inside the dielectric is depicted in Fig. 7, see [37]. R_1 represents the bulk resistance of the device, C_1 is an integer-order capacitor that models the geometry of the BC layer, C_3 is a CPE of order β which describes the non integer phenomena inside the dielectric and C_2, of order α, is another CPE that denotes the double layer capacity between the electrodes and the dielectric. The whole parallel block is mainly responsible for the high-frequencies behaviour, while the C_2 capacitances of the

Journal of Dynamic Systems, Measurement and Control. Received September 30, 2020;
Accepted manuscript posted January 18, 2021. doi:10.1115/1.4049796

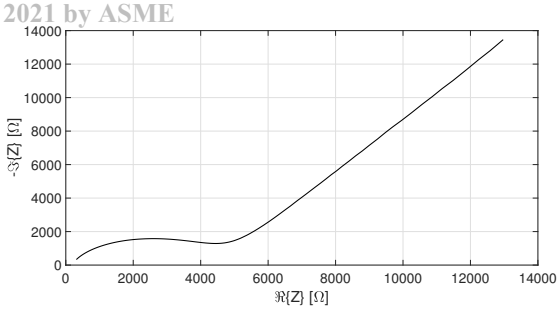

Fig. 6: Nyquist plot of BC-IL-based device first measurement.

low-frequencies one.

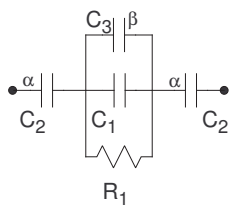

Fig. 7: Proposed Equivalent Electric Circuit Model (EECM) for the BC-IL-based device.

To obtain the impedance parameters of the aforementioned circuit, an identification procedure has been performed by using Genetic Algorithms (GAs) [38, 39]. More specifically, the optimization algorithm has been applied, for each measurement, to a proper cost function. This consists of a weighted combination of both the module and the phase errors, in absolute values, between the real impedance and the corresponding model estimation.

The obtained parameters are reported, in graphical form, in Fig. 8, where the whole set of twenty observations is considered. The vertical dashed lines separate the two groups of measurements described in the previous section. For the sake of comparison, the results of two identifications, performed on a measurement belonging to the first group and one to the second group, are shown in Fig. 9 and 10, respectively. It is possible to observe that the proposed model can fit data belonging to the first group while it is not capable of fitting data belonging to the second set. Similar results have been obtained for all available measurements.

In order to perform quantitative analysis of the fitting capability of the model, a fitting goodness index is used. In particular, the Normalized Root Mean Square Error (NRMSE) has been computed for both the magnitude and phase lag of the available Bode plots. The one's complement has been used to evaluate the fitness goodness.

Considering the acquired signal, in the following x_{acq}, and the corresponding model estimation one, x_{est}, the goodness of fit can be evaluated as:

$$fit = 1 - \frac{\left|x_{acq} - x_{est}\right|}{\left|x_{acq} - \overline{x_{acq}}\right|} \tag{6}$$

where $\bar{\cdot}$ is the mean value of the acquired signal. In the case of study, the acquired signal is obtained by the network analyser, while the estimated one is the Bode response of the identified impedance. Taking into account this expression and evaluating the magnitude (or phase lag) response for both the analysed measurement and the corresponding estimated impedance, it is possible to define the goodness of the identification procedure.

Being eq. (6) the one's complement of the NRMSE, it returns a value between $]-\infty; 1]$, that increases according the quality of fitting. The NRMSE has been computed both for the module and the phase of the device impedance. In the next table, the Goodness Of Fit (GOF) values are reported for all available measurements. From Tab. 1, looking at the fitting qualities for the first ten measurements, it is possible to notice that the identification procedure performs quite well, with fit index values above 95%, for both module and phase. From the 11th measurement and successive ones, although the module is well identified, worse performances are obtained for the phase identification. It can be therefore concluded that the proposed EECM is not able to describe the dynamics of the BC-IL-based FOE for observations belonging to the second group.

5.1 Model validation

A deeper investigation has been performed on the relevance of each capacitance in the model represented in Fig. 7. More specifically, reduced models, obtained by eliminating one capacitance at a time, have been investigated. Results of this analysis will be shown by referring to one measurement (Measurement 1 in G_1).

In particular, the capacitors C_1, C_2 and C_3 have been eliminated one at a time. Reduced EECMs are labelled as *EECM-1*, *EECM-2* and *EECM-3*, respectively. In *EECM-1* and *EECM-3*, the eliminated capacitances (C_1 and C_3, respectively) have been replaced by open circuits. In *EECM-2*, the capacitance C_3 has been replaced by a short circuit. The parameters of the reduced models have been identified and the corresponding model behaviour has been considered.

The Bode diagrams of the reduced models are compared, in Fig. 11, with the experimental Bode diagram of the BC-IL-based FOE.

The model *EECM-1* is able to correctly fit the modulus of the impedance. Unfortunately, the corresponding phase shows an error increasing with the frequency domain (up to about 20 deg). The model *EECM-2* cannot approximate the real behaviour of the BC-IL-based FOE, both in module and phase. Although the module of *EECM-3* fits almost well the module of the real measurement except for the middle frequency range, the phase of the DUT is not satisfactorily reconstructed in all the considered frequency range. Reported

Journal of Dynamic Systems, Measurement and Control. Received September 30, 2020;
Accepted manuscript posted January 18, 2021. doi:10.1115/1.4049796

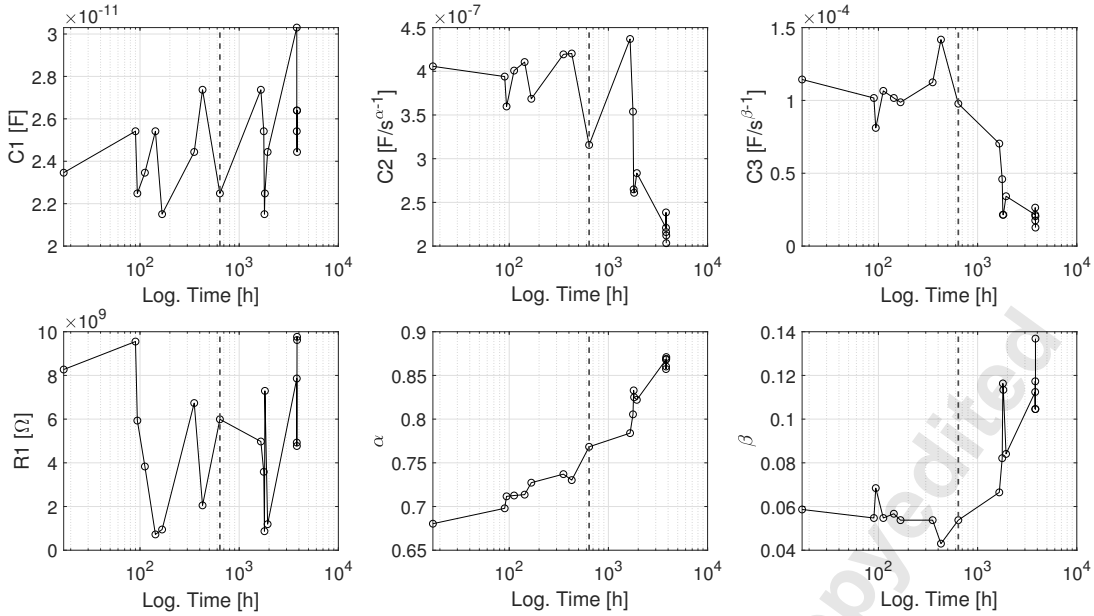

Fig. 8: Parameters values for the proposed equivalent electric circuit model.

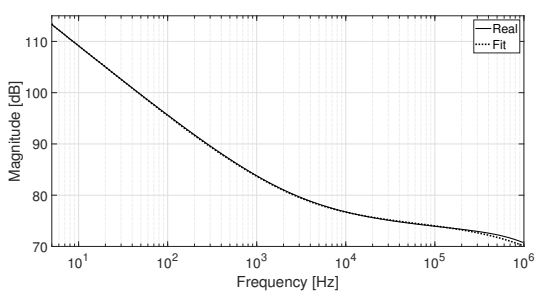

(a) Magnitude

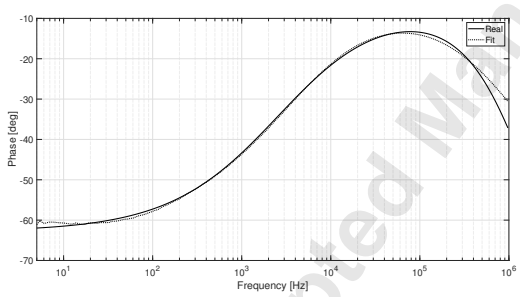

(b) Phase

Fig. 9: Bode diagram of a measurement belonging to G_1 (measurement 1 in Table I).

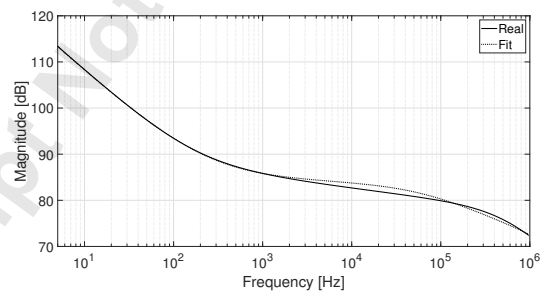

(a) Magnitude

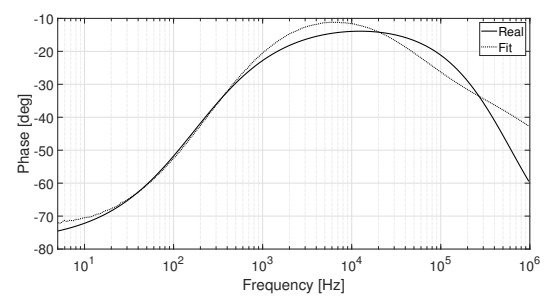

(b) Phase

Fig. 10: Bode diagram of a measurement belonging to G_2 (measurement 17 in Table I).

results show that none of the considered capacitances can be eliminated from the model.

6 Conclusions

In this paper, the complex frequency behaviour of a BC-IL-based FOE device has been deeply analysed in order to model this device as a candidate for fractional-order electronics.

Indeed, it combines both the requirement of being greener and the implementation of new functionalities. Eventually, the device is characterized by low impedance values at low frequencies.

The composite has been characterized at constant temperature and humidity working conditions. The proposed model allows to validate the fractional-order nature of the

Journal of Dynamic Systems, Measurement and Control. Received September 30, 2020;
Accepted manuscript posted January 18, 2021. doi:10.1115/1.4049796

Measurement	GOF - Module	GOF - Phase
1 - 0*h*	0.9641	0.9578
2 - 17 *h*	0.9850	0.9514
3 - 90 *h*	0.9920	0.9390
4 - 94 *h*	0.9914	0.9582
5 - 112 *h*	0.9922	0.9538
6 - 143 *h*	0.9928	0.9486
7 - 167 *h*	0.9855	0.9505
8 - 352 *h*	0.9916	0.9554
9 - 427 *h*	0.9885	0.9265
10 - 639 *h*	0.9347	0.9587
11 - 1654 *h*	0.9888	0.8785
12 - 1770 *h*	0.9749	0.8890
13 - 1798 *h*	0.9860	0.8604
14 - 1817 *h*	0.9773	0.8514
15 - 1935 *h*	0.9766	0.8449
16 - 3808 *h*	0.9868	0.8020
17 - 3809 *h*	0.9839	0.8383
18 - 3814 *h*	0.9875	0.7843
19 - 3831 *h*	0.9902	0.7997
20 - 3832 *h*	0.9838	0.7702

Table 1: Goodness of fit values for the performed measurements.

device.

Investigations were performed for about six months. After about one month the device lost its stability and a stable behaviour was not recovered. Further research activity is required to understand the cause of such instability. More specifically, investigations are needed to study and understand how several and different ILs can solve this issue, while modulating the behaviour of the proposed fractional-order electronics.

As a future research activity, the possibility of using eco-friendly ILs, whose ecological impact should be lower than the commercial one used until now, will be investigated. In this way a completely eco-friendly device can be realized.

Acknowledgements

This article is based upon work from COST Action CA15225 "Fractional order systems analysis, synthesis and their importance for future design)", supported by COST (European Cooperation in Science and Technology).

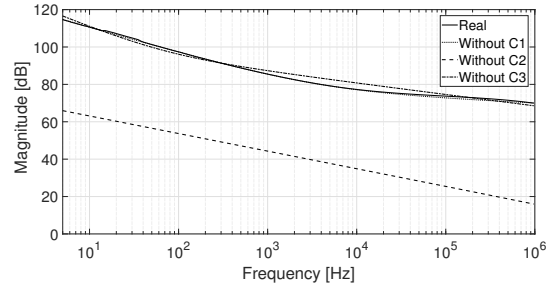

(a) Magnitude

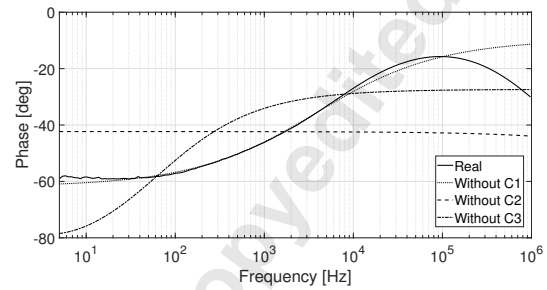

(b) Phase

Fig. 11: Bode diagram of the reduced EECM without C_1, C_2 and C_3, respectively (measurement 1 in Table I).

References

[1] Guterres, A., 2020. International Mother Earth Day. "https://www.un.org/en/observances/earth-day/message". Online; accessed 05 May 2020.

[2] Baldé, C. P., Forti, V., Gray, V., Kuehr, R., and Stegmann, P., 2017. "The global e-waste monitor – 2017". *United Nations University (UNU), International Telecommunication Union (ITU) & International Solid Waste Association (ISWA), Bonn/Geneva/Vienna*.

[3] IEWD-About, 2018. Waste electrical and electronic equipment directive. https://weee-forum.org/iewd-about/. Online; accessed 05 May 2020.

[4] Press-Release, 2019. Un report: Time to seize opportunity, tackle challenge of e-waste. https://www.unenvironment.org/news-and-stories/press-release/un-report-time-seize-opportunity/-tackle-challenge-e-waste. Online; accessed 05 May 2020.

[5] Jozala, A., de Lencastre-Novaes, L., Lopes, A., de Carvalho Santos-Ebinuma, V., Mazzola, P., Pessoa-Jr., A., Grotto, D., Gerenutti, M., and Chaud, M., 2016. "Bacterial nanocellulose production and application: a 10-year overview". *Appl. Microb. Biotech.,* **100**(5), pp. 2063 – 2072.

[6] Iguchi, M., Yamanaka, S., and Budhiono, A., 2000. "Bacterial cellulose - a masterpiece of nature's arts". *J. Mat. Sci.,* **35**(2), pp. 261 – 270.

[7] Grau, G., Frazier, E., and Subramanian, V., 2016. "Printed unmanned aerial vehicles using paper-based

Journal of Dynamic Systems, Measurement and Control. Received September 30, 2020;
Accepted manuscript posted January 18, 2021. doi:10.1115/1.4049796

electroactive polymer actuators and organic ion gel transistors". *Microsys. Nanoeng.,* **2**.

[8] Trigona, C., Graziani, S., Pasquale, G. D., Pollicino, A., Nis, R., and Licciulli, A., 2020. "Green energy harvester from vibrations based on bacterial cellulose". *Sensors,* **20**(136).

[9] Wang, Y., Song, P., Li, X., Ru, C., Ferrari, G., Balasubramanian, P., Amabili, M., Sun, Y., and Liu, X., 2018. "A paper-based piezoelectric accelerometer". *Micromachines,* **9**(1).

[10] Pasquale, G. D., Graziani, S., Pollicino, A., and Trigona, C., 2019. "Green inertial sensors based on bacterial cellulose". *IEEE Sensors Applications Symposium, Conference Proceedings*(8706112).

[11] Trigona, C., Graziani, S., Pasquale, G. D., Pollicino, A., Nisi, R., and Licciulli, A., 2020. "Green energy harvester from vibrations based on bacterial cellulose". *Sensors,* **20**(1).

[12] Wang, F., Jeon, J., Park, S., Kee, C., Kim, S., and Oh, I., 2016. "A soft biomolecule actuator based on a highly functionalized bacterial cellulose nano-fiber network with carboxylic acid groups". *Soft Matter,* **12**(1), pp. 246 – 254.

[13] Zheng, Y., Yang, J., Zheng, W., Wang, X., Xiang, C., Tang, L., Zhang, W., Chen, S., and Wang, W., 2013. "Synthesis of flexible magnetic nanohybrid based on bacterial cellulose under ultrasonic irradiation". *Mat. Sci. Eng. C,* **33**(4), pp. 2407 – 2412.

[14] Caponetto, R., Pasquale, G. D., Graziani, S., Murgano, E., and Pollicino, A., 2019. "Realization of green fractional order devices by using bacterial cellulose". *AEU – Int. J. of Elec. and Comm.,* **112**(1), pp. 246 – 254.

[15] Buscarino, A., Caponetto, R., Graziani, S., and Murgano, E., 2020. "Realization of fractional order circuits by a constant phase element". *European J. of Control,* **54**, pp. 64 – 72.

[16] Caponetto, R., Dongola, G., Fortuna, L., and Petras, I., 2010. *Fractional Order Systems: Modelling and Control Applications*, Vol. 72. World Scientific Book, World Scientific Series On Nonlinear Science Series A.

[17] Monje, C. A., Chen, Y., Vinagre, B. M., Xue, D., and Feliu-Batlle, V., 2010. *Fractional-order Systems and Controls: Fundamentals and Applications*. Springer.

[18] Tsirimokou, G., Psychalinos, C., and Elwakil, A., 2017. *Design of CMOS analog integrated fractional-order circuits applications in medicine and biology*. Springer International Publishing.

[19] Adhikary, A., Shil, A., and Biswas, K., 2020. "Realization of foster structure-based ladder fractor with phase band specification". *Circuits, Systems, and Signal Processing,* **39**(5), pp. 2272 – 2292.

[20] Caponetto, R., Pasquale, G. D., Graziani, S., Murgano, E., Pollicino, A., and Trigona, C., 2020. "Green fractional order elements based on bacterial cellulose and ionic liquids". *Proceedings I2MTC 2020 - IEEE Int. Instrumentation and Meas. Conf., I2MTC 2020.*

[21] Oldham, K. B., and Spanier, J., 2006. *The Fractional Calculus: Theory and Applications of Differentiation and Integration to Arbitrary Order*. Elsevier.

[22] Sun, H., Zhang, Y., Baleanu, D., Chen, W., and Chen, Y., 2018. "A new collection of real world applications of fractional calculus in science and engineering". *Communication in Nonlinear Science and Numerical Simulation,* **64**, pp. 213 – 231.

[23] Keyser, R. D., Muresan, C., and Ionescu, C., 2016. "A novel auto-tuning method for fractional order pi/pd controllers". *ISA Transactions,* **62**, pp. 268 – 275.

[24] Coronel-Escamilla, A., Gómez-Aguilar, J., Torres, L., Escobar-Jimènez, R., and Olivares-Peregrino, V., 2018. "Fractional observer to estimate periodical forces". *ISA Transactions,* **82**, pp. 30 – 41.

[25] Caponetto, R., Dongola, G., Maione, G., and Pisano, A., 2014. "Integrated technology fractional order proportional-integral-derivative design". *Journal of Vibration and Control,* **20**(7), pp. 1066 – 1075.

[26] Solís-Péreza, J., Gómez-Aguilar, J., Torres, L., Escobar-Jiménez, R., and Reyes-Reyes, J., 2019. "Fitting of experimental data using a fractional kalman-like observer". *ISA Transactions,* **88**(1), pp. 153 – 169.

[27] Fallahgoul, H., Focardi, S., and Fabozzi, F., 2016. *Fractional Calculus and Fractional Processes with Applications to Financial Economics Theory and Application*. Academic Press.

[28] Beltempo, A., Zingales, M., Bursi, O., and Deseri, L., 2018. "International journal of solids and structures". *Advanced Water Resources,* **138**, pp. 13 – 23.

[29] Shah, Z., Kathjoo, M., Khanday, F., Biswas, K., and Psychalinos, C., 2019. "A survey of single and multi-component fractional-order elements (foes) and their applications". *Microelectron J,* **84**, pp. 9 – 25.

[30] Elshurafa, M., Almadhoun, N., Salama, K., and Alshareef, H., 2013. "Microscale electrostatic fractional capacitors using reduced graphene oxide percolated polymer composites". *Appl. Phys. Lett.,* **102**(23).

[31] Buscarino, A., Caponetto, R., Pasquale, G. D., Fortuna, L., Graziani, S., and Pollicino, A., 2018. "Carbon black based capacitive fractional order element towards a new electronic device". *Int. J. Electron. Commun. (AEU),* **84**, pp. 307 – 312.

[32] Agambayev, A., Farhat, M., Patole, S. P., Hassan, A. H., Bagci, H., and Salama, K., 2018. "An ultra-broadband single-component fractional-order capacitor using mos2-ferroelectric polymer composite". *Appl. Phys. Lett.,* **113**(9).

[33] Adhikary, A., Khanra, M., Sen, S., and Biswas, K., 2015. "Realization of a carbon nanotube based electrochemical fractor". *Proceedings ISCAS 2015 - IEEE International Symposium on Circuits and Systems*, pp. 2329 – 2332.

[34] Caponetto, R., Graziani, S., Pappalardo, F., and Sapuppo, F., 2013. "Experimental characterization of ionic polymer-metal composite as a novel fractional order element". *Adv. Math. Phys.*

[35] Remsing, R. C., Hernandez, G., Swatloski, R. P., Massefski, W. W., Rogers, R. D., and Moyna, G., 2008. "Solvation of carbohydrates in n,n'-dialkylimidazolium

Journal of Dynamic Systems, Measurement and Control. Received September 30, 2020;
Accepted manuscript posted January 18, 2021. doi:10.1115/1.4049796

ionic liquids: a multinuclear nmr spectroscopy study". *J. Phys. Chem. B,* **112**(35), pp. 4202 – 4206.

[36] Arof, A. K., Amirudin, S., Yusof, S. Z., and Noor, I. M., 2014. "A method based on impedance spectroscopy to determine transport properties of polymer electrolytes". *Phys. Chem. Chem. Phys.,* **16**, pp. 1856 – 1867.

[37] Qian, X., Gu, N., Cheng, Z., Yang, X., Wang, E., and Dong, S., 2001. "Methods to study the ionic conductivity of polymeric electrolytes using a.c. impedance spectroscopy". *J Solid State Electrochem.,* **6**(35), pp. 8 – 15.

[38] Goldberg, D., 1989. *Genetic Algorithms in Search, Optimization, and Machine Learning*. Addison-Wesley Professional.

[39] Chipperfield, A. J., Fleming, P. J., and Fonseca, C. M., 1994. "Genetic algorithm tools for control systems engineering". *Proc. Adaptive Computing in Engineering Design and Control*, pp. 128 – 123.